Neurobiology of Aging 115 (2022) 12–19

Contents lists available at ScienceDirect

Neurobiology of Aging

journal homepage: www.elsevier.com/locate/neuaging.org

Differential effects of white matter hyperintensities and regional amyloid deposition on regional cortical thickness

Chin Hong Tan[a,b,*], Justin Chew[c,d], Liwen Zhang[e,f], Balázs Gulyás[b], Christopher Chen[f,g], for the Alzheimer's Disease Neuroimaging Initiative

[a] Division of Psychology, Nanyang Technological University, Singapore
[b] Lee Kong Chian School of Medicine, Nanyang Technological University, Singapore
[c] Department of Geriatric Medicine, Tan Tock Seng Hospital, Singapore
[d] Institute of Geriatrics and Active Ageing, Tan Tock Seng Hospital, Singapore
[e] Memory and Aging Center, Department of Neurology, Weill Institute for Neurosciences, University of California, San Francisco, San Francisco, California, USA
[f] Department of Pharmacology, Yong Loo Lin School of Medicine, National University of Singapore, Singapore
[g] Memory Aging and Cognition Centre, National University Health System, Yong Loo Lin School of Medicine, National University of Singapore, Singapore

ARTICLE INFO

Article history:
Received 1 November 2021
Revised 12 March 2022
Accepted 17 March 2022
Available online 26 March 2022

Keywords:
Amyloid
Cerebral cortical thinning
White matter hyperintensities (WMH)
Alzheimer's disease (AD)
cerebrovascular disease

ABSTRACT

White matter hyperintensities (WMH) and β-amyloid (Aβ) accumulation have both been linked to neurodegeneration in Alzheimer's disease (AD). However, the independent effects of global WMH and regional Aβ on the corresponding regional cortical thickness have not been investigated. Here, we evaluated 280 cognitively normal (CN), 450 mild cognitive impairment (MCI), and 63 individuals with AD dementia separately. In CN individuals, only WMH was associated with lower cortical thickness in fronto-temporal regions, independent of regional Aβ deposition in the corresponding cortical regions. In MCI individuals, the spatial pattern of independent WMH associations was predominantly in temporal and cingulate regions, while independent regional Aβ associations were now evident in temporal regions. No regional interactions were found. In non-demented individuals and MCI individuals alone, we found that global WMH, composite regional Aβ burden and cortical thickness in AD-associated regions all independently predicted progression to AD dementia. Our findings suggest that the independent effects of global WMH and regional Aβ on regional cortical thickness are spatially different, converging in temporal regions in MCI individuals.

1. Introduction

There has been greater appreciation that mixed dementia is the norm, with Alzheimer's disease pathology most likely to be found alongside another neurodegenerative and vascular pathology, or with at least one vascular pathology (Boyle et al., 2018). Aligning with these pathological evidence, studies have sought to establish the independent and interactive effects of AD-associated β-amyloid (Aβ) burden and white matter hyperintensities (WMH) of presumed vascular origins on magnetic resonance imaging (MRI) measures of neurodegeneration (Bos et al., 2017; Parker et al., 2020; Yassi et al., 2020). While the relationship between WMH and neurodegeneration both cross-sectionally (Du et al., 2005; Habes et al., 2016; Vipin et al., 2018) and longitudinally (Dadar et al., 2022; Kim et al., 2020; Lao and Brickman, 2018; Rizvi et al., 2021) are well-established, the relationships between global WMH, *regional* Aβ accumulation and *regional* neurodegeneration are not well understood (De Guio et al., 2020). This may be due to the usage of cerebrospinal fluid (CSF) measures of Aβ which does not allow for regional analyses or the usage of a global assessment of Aβ positron emission tomography (PET) standard uptake value ratio (SUVR) or binary positivity to quantify Aβ burden in the brain.

Data used in preparation of this article were obtained from the Alzheimer's Disease Neuroimaging Initiative (ADNI) database (adni.loni.usc.edu). As such, the investigators within the ADNI contributed to the design and implementation of ADNI and/or provided data but did not participate in analysis or writing of this report. A complete listing of ADNI investigators can be found at: http://adni.loni.usc.edu/wp-content/uploads/how_to_apply/ADNI_Acknowledgement_List.pdf

* Corresponding author at: Chin Hong Tan, Nanyang Technological University, 48 Nanyang Avenue S639818, Singapore, Tel: +65 65921581.
E-mail address: chinhong.tan@ntu.edu.sg (C.H. Tan).

0197-4580/$ – see front matter © 2022 Elsevier Inc. All rights reserved.
https://doi.org/10.1016/j.neurobiolaging.2022.03.013

Table 1
Demographics.

	CN (n = 280)	MCI (n = 450)	Dementia (n = 64)
Age, M ± SD	73.37 (6.24)	71.49 (7.49)	73.33 (8.75)
Education, M ± SD	16.45 (2.64)	16.27 (2.68)	15.50 (2.48)
Sex, Female (%)	154 (55.00)	201 (44.67)	33 (51.56)
Racial category, White (%)	253 (90.36)	419 (95.33)	60 (93.75)
APOE e4 dosage (0/1/2)	195/78/7	226/174/50	20/30/14
Log WMH volume, M ± SD	1.03 (1.10)	1.19 (1.15)	1.57 (1.04)
Florbetapir SUVR, M ± SD	1.11 (0.18)	1.23 (0.23)	1.45 (0.20)
Cortical Thickness in AD -associated regions, mm, M ± SD	2.74 (0.13)	2.67 (0.18)	2.41 (0.17)

Key: AD, Alzheimer's disease; WMH, White matter hyperintensity; SUVR, Standard uptake value ratio.

Given the confluence of evidence showing the presence of amyloid staging regional patterns (Grothe et al., 2017; Mattsson et al., 2019; Pfeil et al., 2021) alongside known regional vulnerabilities to AD-associated neurodegeneration in select cortical regions (Dickerson et al., 2009; Schwarz et al., 2016), regional analyses may provide additional information beyond global assessment of Aβ burden and/or neurodegeneration. Further, it is unknown if these regional spatial relationships are similar across disease stages. Therefore, the current study takes a regional approach by investigating the differential effects i.e., independent contributions and interactive effects of global WMH and regional amyloid PET deposition on the *corresponding* regional cortical thickness in cognitively normal (CN) individuals, individuals with mild cognitive impairment (MCI), and individuals with AD dementia separately. In addition, while global WMH has been found to be associated with greater progression to dementia (Benedictus et al., 2015; Heng et al., 2021; Kim et al., 2015), whether global WMH, regional Aβ burden and regional neurodegeneration all contribute independently to clinical progression are unknown.

In sum, using a series of regional and survival analyses, this study aims to determine 1) the differential contribution (i.e., the independent and interaction effects) of global WMH and regional cortical Aβ deposition on regional cortical thickness in CN, MCI, and AD dementia individuals separately and 2) the independent effects of global WMH, composite regional Aβ and cortical thickness in AD-associated regions on progression to AD dementia in non-demented individuals.

2. Methods

2.1. Participants and clinical characterization

Data used in the preparation of this article were obtained from the ADNI database (adni.loni.usc.edu). The ADNI was launched in 2003 as a public-private partnership, led by Principal Investigator Michael W. Weiner, MD. The primary goal of the ADNI has been to test whether serial MRI, PET, other biological markers, and clinical and neuropsychological assessment can be combined to measure the progression of mild cognitive impairment (MCI) and early Alzheimer's disease. Here, we evaluated 280 cognitively normal (CN) individuals, 450 individuals with MCI, and 64 individuals with AD dementia as determined by a global Clinical Dementia Rating (CDR) of 0, 0.5 and $\geq$ 1 respectively. Only participants who had complete white matter hyperintensity, florbetapir SUV, and cortical thickness data that were already processed and available from the ADNI database were included in the study. The resultant sample who had all available data were all from ADNIGO/2. Sample demographics are summarized in Table 1.

2.2. Neuroimaging acquisition and processing

In brief, structural MRI scans were acquired using a 3T scanner. Cortical reconstruction and volumetric segmentation were performed with the Freesurfer 5.1 image analysis suite, which is documented and freely available for download online (http://surfer.nmr.mgh.harvard.edu). The technical details of the procedure have previously been described (Dale et al., 1999; Fischl and Dale, 2000). Regional cortical thickness measures were delineated based on the Desikan-Killany atlas (Desikan et al., 2006) and estimated intracranial volume (ICV) data were also derived using the Freesufer analytic pipeline.

The WMH data were derived from the segmentation of 3D T1 and T2-FLAIR sequences using a Bayesisan approach. FLAIR inhomogeneity corrections were implemented using a histogram normalizing method (DeCarli et al., 1996) and all image segmentations were done in a common template space (DeCarli et al., 2005). Only global WMH data were available in the ADNI database for analyses in the current study.

Florbetapir (18F-AV45) PET images data were co-registered, averaged, interpolated and smoothed. This was followed by co-registration with their 3D T1 that has been processed with Freesurfer 7.1.1 to delineate and compute regional florbetapir SUVRs in cortical regions based on the Desikan-Killany atlas (Desikan et al., 2006). The processing steps of the florbetapir scans have been previously described in greater detail (Landau et al., 2013; Landau et al., 2012).

2.3. Statistical analysis

First, we used linear regression to investigate the basic relationships between global WMH and regional Aβ, controlling for age, sex, education, categorical APOE e4 dosage, and estimated ICV. The white matter hyperintensities volume were log-transformed prior to statistical analysis due to non-normality of the distribution (Tan et al., 2019). Regional florbetapir (PET ^{18}F-AV45) SUVRs were obtained by averaging left and right hemispheres' SUVs in 34 cortical regions of interests (ROIs) derived from the Desikan-Killiany Freesurfer atlas (Desikan et al., 2006) and the averaged SUV in each cortical region was then normalized by the whole cerebellum florbetapir SUV. Next, we investigated the independent i.e., additive contribution of global WMH and regional Aβ on the *corresponding* regional cortical thickness, controlling for the same covariates. WMH and regional Aβ were used as predictors, regional cortical thickness as criterion variables. The corresponding 34 regional Freesurfer cortical thickness were also obtained by averaging thickness measures for the left and right hemispheres. We cor-

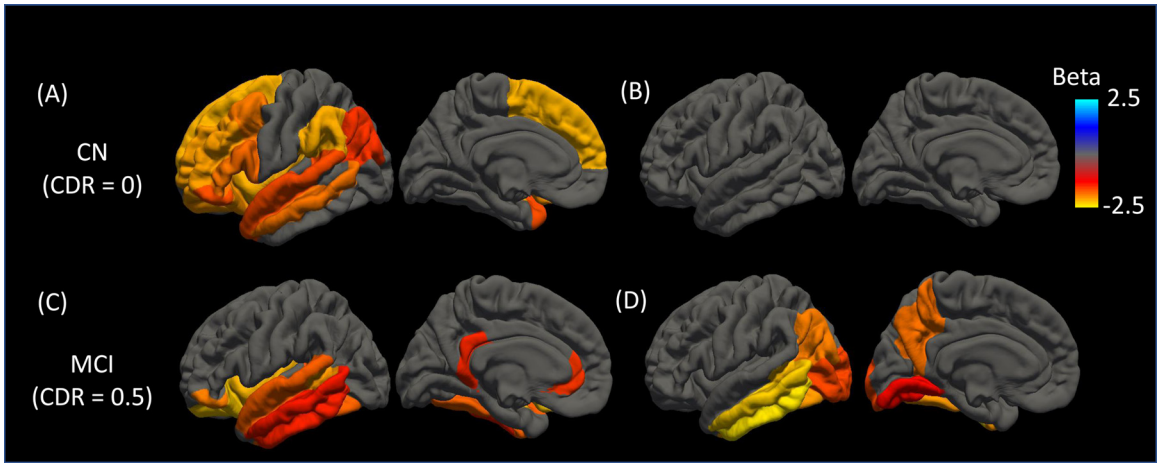

Fig. 1. Independent associations of (A) WMH and (B) regional amyloid SUVR on regional cortical thickness in cognitively normal individuals and (C & D) for individuals with mild cognitive impairment ($q < 0.05$). No statistically significant associations were found in individuals with AD dementia.

Table 2
Independent associations of white matter hyperintensity and regional amyloid SUVR on regional cortical thickness in cognitively normal individuals.

Region of Interest (ROI)	White Matter Hyperintensity		Florbetapir SUVR	
	Beta	FDR-adjusted q	Beta	FDR-adjusted q
Banks of the superior temporal sulcus	-0.120	0.097	-0.019	0.837
Caudal anterior cingulate	-0.131	0.071	-0.093	0.302
Caudal middle frontal	**-0.188**	**0.013**	0.112	0.207
Cuneus	0.000	0.996	0.030	0.821
Entorhinal	-0.062	0.376	0.077	0.447
Fusiform	-0.112	0.105	0.035	0.748
Inferior parietal	**-0.152**	**0.032**	0.060	0.572
Inferior temporal	-0.123	0.087	-0.111	0.207
Isthmus cingulate	-0.107	0.128	-0.093	0.302
Lateral occipital	-0.118	0.093	0.071	0.447
Lateral orbitofrontal	**-0.201**	**0.009**	0.051	0.644
Lingual	-0.124	0.079	0.134	0.147
Medial orbitofrontal	-0.083	0.248	0.053	0.644
Middle temporal	**-0.185**	**0.010**	-0.014	0.843
Parahippocampal	-0.084	0.248	-0.045	0.674
Paracentral	-0.016	0.848	0.124	0.193
Pars opercularis	**-0.180**	**0.016**	0.020	0.837
Pars orbitalis	**-0.166**	**0.022**	0.017	0.837
Pars triangularis	**-0.186**	**0.014**	0.019	0.837
Pericalcarine	0.029	0.729	-0.018	0.837
Postcentral	-0.006	0.952	0.141	0.147
Posterior cingulate	-0.100	0.178	-0.027	0.837
Precentral	-0.109	0.123	0.139	0.147
Precuneus	-0.077	0.273	0.046	0.674
Rostral anterior cingulate	-0.093	0.205	0.062	0.572
Rostral middle frontal	**-0.205**	**0.009**	0.123	0.193
Superior frontal	**-0.216**	**0.007**	0.118	0.193
Superior parietal	-0.020	0.810	0.138	0.147
Superior temporal	-0.164	0.014	0.086	0.302
Supramarginal	-0.213	0.007	0.135	0.147
Frontal pole	-0.065	0.375	0.079	0.447
Temporal pole	**-0.166**	**0.022**	0.154	0.147
Transverse temporal	-0.091	0.205	0.117	0.193
Insula	**-0.214**	**0.009**	-0.003	0.958

Bold = FDR-adjusted $q < 0.05$

rected for multiple comparisons at a false discovery rate (FDR) of $q < .05$ based on a total of 34 linear regressions conducted in all ROIs. Predictors and criterion variables were centered and scaled prior to analysis.

For interaction analyses, we tested whether the interaction of global WMH with regional Aβ was associated with regional cortical thickness. In addition, we derived composite cortical thickness and composite Aβ measures by averaging them in known AD-associated regions (entorhinal, para-hippocampus, inferior parietal, pars opercularis, pars orbitalis, pars triangularis, inferior temporal, temporal pole, precuneus, supramarginal gyrus, superior parietal, and superior frontal cortex (Dickerson et al., 2009)). We then tested whether there was an interaction between global WMH and composite Aβ on composite cortical thickness. These interaction analyses included all base terms and covariates (age, sex, education, categorical APOE e4 dosage, and ICV). All analyses were conducted separately in the 3 diagnostic groups i.e., CN, MCI and individuals with AD dementia.

Table 3
Independent associations of white matter hyperintensity and regional amyloid SUVR on regional cortical thickness in mild cognitively impaired individuals.

Region of Interest (ROI)	White Matter Hyperintensity		Florbetapir SUVR	
	Beta	FDR-adjusted q	Beta	FDR-adjusted q
Banks of the superior temporal sulcus	**-0.203**	**1.06E-03**	**-0.220**	**1.54E-04**
Caudal anterior cingulate	-0.105	1.09E-01	0.057	4.73E-01
Caudal middle frontal	-0.087	1.76E-01	-0.070	4.39E-01
Cuneus	0.092	1.76E-01	-0.050	5.02E-01
Entorhinal	-0.119	5.57E-02	0.056	4.51E-01
Fusiform	**-0.176**	**2.13E-03**	**-0.203**	**1.79E-04**
Inferior parietal	-0.033	6.11E-01	**-0.190**	**1.72E-03**
Inferior temporal	**-0.143**	**1.77E-02**	**-0.240**	**5.84E-05**
Isthmus cingulate	**-0.146**	**1.77E-02**	-0.094	1.93E-01
Lateral occipital	-0.032	6.11E-01	**-0.162**	**4.36E-03**
Lateral orbitofrontal	**-0.226**	**7.09E-04**	-0.056	4.73E-01
Lingual	-0.050	4.42E-01	**-0.130**	**2.85E-02**
Medial orbitofrontal	-0.058	3.88E-01	-0.086	3.22E-01
Middle temporal	**-0.139**	**2.05E-02**	**-0.228**	**1.03E-04**
Parahippocampal	-0.099	1.27E-01	0.044	5.73E-01
Paracentral	0.130	5.01E-02	0.001	9.78E-01
Pars opercularis	-0.046	4.93E-01	-0.034	6.98E-01
Pars orbitalis	**-0.189**	**2.13E-03**	-0.060	4.51E-01
Pars triangularis	-0.067	2.98E-01	0.011	9.12E-01
Pericalcarine	0.100	1.30E-01	-0.020	8.46E-01
Postcentral	-0.017	7.67E-01	0.027	7.71E-01
Posterior cingulate	-0.018	7.67E-01	-0.064	4.51E-01
Precentral	0.037	5.68E-01	0.065	4.39E-01
Precuneus	0.012	8.16E-01	**-0.183**	**2.95E-03**
Rostral anterior cingulate	**-0.153**	**1.77E-02**	0.003	9.78E-01
Rostral middle frontal	-0.082	2.20E-01	-0.017	8.51E-01
Superior frontal	-0.069	2.80E-01	-0.038	6.56E-01
Superior parietal	0.076	2.56E-01	-0.020	8.46E-01
Superior temporal	**-0.174**	**2.13E-03**	-0.085	2.23E-01
Supramarginal	-0.126	5.01E-02	-0.061	4.51E-01
Frontal pole	-0.027	6.89E-01	-0.003	9.78E-01
Temporal pole	-0.117	5.97E-02	0.116	6.25E-02
Transverse temporal	-0.114	7.00E-02	0.038	6.54E-01
Insula	**-0.218**	**7.51E-04**	-0.017	8.51E-01

Bold = FDR-adjusted $q < 0.05$

Lastly, we investigated the independent effects of global WMH, composite Aβ, and composite cortical thickness on progression to AD dementia using Cox proportional hazards model with time to event indicated by age of AD dementia onset (Tan et al., 2017). We resolved 'ties' using the Breslow method and covaried for age, sex, education, APOE e4 dosage, ICV. We additionally covaried for ICV stratified into quartiles (Tan et al., 2018) to adjust for violations of Cox proportional hazards assumptions by ICV. Conclusions were unchanged regardless of whether this additional covariate was included. None of the variables in the final survival analysis models violated the Cox proportional hazards assumption as determined using scaled Schoenfeld residuals. Due to low conversion rates ($n = 5$) to AD dementia for CN individuals, these survival analyses were only conducted in all non-demented individuals (CN and MCI together) and in MCI individuals alone. All statistical analyses were conducted using R 4.1.0.

3. Results

3.1. Basic relationships between WMH and regional Aβ

In CN individuals, global WMH was associated with Aβ SUVR in 22 out of 34 regions at uncorrected $p < 0.05$ (Supplemental Figure 1). These associations were strongest in frontoparietal regions such as the superior frontal, superior parietal, precuneus, postcentral, cuneus, and inferior parietal cortices. However, none of these regions survived multiple correction at FDR-adjusted $q < 0.05$ (Supplemental Table 1). In MCI individuals, WMH was only associated with superior parietal cortex ($\beta = 0.10$, $p < 0.05$) but this association also did not survive correction for multiple comparisons. No associations were found even at uncorrected $p < 0.05$ for individuals with AD dementia.

3.2. Independent effects of WMH and regional Aβ on regional cortical thickness

In CN individuals, higher WMH volume was significantly associated with lower regional cortical thickness in 13 out of the 34 ROIs (Fig. 1A, Table 2), corrected for multiple comparisons at FDR-adjusted $q < 0.05$, even after accounting for the corresponding regional Aβ and other covariates. The effects were found predominantly in fronto-temporal regions. In comparison, none of the regional Aβs were associated with the corresponding regional cortical thickness in the same model containing WMH and other covariates (Fig. 1B, Table 2).

In MCI individuals, the number of regions that higher WMH was independently associated with cortical thickness was reduced to 10 of 34 ROIs (Fig. 1C, Table 3), also corrected for multiple comparisons at FDR-adjusted $q < 0.05$. The frontal associations were no longer statistically significant while the associations with temporal regions persisted. In addition, WMH associations with regions in the cingulate cortex emerged in these MCI patients. In the same model, higher regional Aβs were now independently associated with lower cortical thickness in 8 corresponding ROIs (Fig. 1D, Table 3). These associations were strongest in the temporal regions and were also found in regions such as the precuneus and inferior parietal regions. In individuals with AD dementia, WMH was not independently associated with regional cortical thickness in all regions. Although Aβ SUVR was independently associated with cortical thickness in 4 regions (fusiform, supramarginal, precuneus, and

postcentral cortex) at uncorrected $p < 0.05$, no statistically significant associations were found at FDR-adjusted $q < 0.05$ (Supplemental Table 2).

3.3. Interactions of WMH and regional Aβ on regional cortical thickness

In all diagnostic groups, there was no evidence of any interactions between WMH and regional Aβ on regional cortical thickness (FDR-adjusted $q > 0.05$). We also did not find a significant interaction of WMH with composite Aβ on composite cortical thickness for CN ($\beta = 0.006$, SE = 0.062, $p > 0.05$), MCI ($\beta = 0.012$, SE = 0.044, $p > 0.05$), and individuals with AD dementia ($\beta = 0.244$, SE = 0.154, $p > 0.05$).

3.4. Independent effects of WMH, Aβ and cortical thickness on progression to AD dementia

In non-demented individuals, 116 individuals (5 CN and 111 MCI) progressed to AD dementia. Higher WMH (Hazard ratio (HR) = 1.39, 95% CI = 1.11 – 1.73), higher composite Aβ SUVR (HR = 2.74, 95% CI = 2.23 – 3.36), and lower composite thickness (HR = 2.58, 95% CI = 2.11 – 3.56) predicted progression to AD dementia. Similarly, in MCI individuals only, higher WMH (HR = 1.36, 95% CI = 1.09 – 1.70), higher composite Aβ SUVR (HR = 2.71, 95% CI = 2.15 – 3.43), and lower composite thickness (HR = 2.31, 95% CI = 1.84 – 2.90) all predicted progression to AD dementia.

4. Discussion

The findings presented in the current study supports the differential spatial effects of WMH and regional Aβ burden on regional cortical thickness in CN and MCI individuals, and that WMH are independently associated with progression to AD dementia beyond regional cortical Aβ and neurodegeneration. In CN individuals, greater global WMH was associated with lower regional cortical thickness in predominantly fronto-temporal regions, independent of regional cortical Aβ burden. Although previous studies have reported fronto-temporal associations of WMH and cortical thickness in non-demented individuals without accounting for Aβ burden (Tuladhar et al., 2015), here we additionally show that this fronto-temporal pattern of association is not only independent of fronto-temporal cortical Aβ accumulation, but also specific to CN individuals only. Our analysis in CN and MCI individuals separately revealed that in MCI individuals, the spatial pattern of this independent regional association shifts from a fronto-temporal pattern to one that retains temporal but not frontal regions, and also now includes the emergence of select cingulate (rostral anterior and isthmus) regions. In individuals with AD dementia, none of the regional associations were statistically significant.

The independent associations between cortical thickness in the cingulate and global WMH in MCI individuals have also been found in a prior study involving only cognitively impaired individuals adjusting for global Pittsburgh compound (PiB) retention ratios (Ye et al., 2015) and may reflect the key role of the anterior cingulate cortex (ACC) in the manifestation of neuropsychiatric symptoms (NPS) that are commonly found in individuals with dementia (Lyketsos et al., 2002; Zhao et al., 2016) which have been linked to underlying mixed cerebrovascular and neurodegenerative pathologies, particularly in more severe disease stages (Kan et al., 2022; Misquitta et al., 2020). The isthmus cingulate also has strong structural and functional connections with the default mode network (Zhu et al., 2013) and its association with WMH independent of Aβ in the current study may reflect the damage to structural white matter fibers due to cerebrovascular disease. Our current study adds to the literature by suggesting that these cingulate associations are independent of regional Aβ and likely only becomes salient in MCI patients, but not in CN individuals.

While higher regional Aβ was not associated with lower regional cortical thickness independent of WMH in CN individuals, these associations surfaced in temporal regions, precuneus, and inferior parietal cortex in MCI individuals. These are well-established AD-associated regions associated with the neurodegenerative process in Alzheimer's disease (Dickerson et al., 2009) and parallels a previous study involving only cognitively impaired individuals using global PiB (Ye et al., 2015). Our additional finding that the presence of associations of WMH but not regional Aβ with regional cortical thickness in CN individuals are also consistent with longitudinal findings in individuals across the disease spectrum showing that WMH but not CSF $A\beta_{1-42}$ levels was associated with changes in grey matter volume (Dadar et al., 2020). The convergence of the independent effects of both WMH and regional Aβ burden in the cortical thickness of temporal regions in MCI individuals may reflect that even at mild cognitive impairment stages, neurodegeneration in temporal regions may be influenced by both cerebrovascular and Aβ pathologies. Temporal regions are known to be vulnerable to greater tau accumulation in AD (Ossenkoppele et al., 2016; Sanchez et al., 2021), and while tau and Aβ show distinct patterns of neurodegeneration, the inferior-lateral temporal lobe in particular has been shown to be a convergence zones of both pathologies (Sepulcre et al., 2016). The absence of statistically significant associations in individuals with AD dementia in the current study may also be suggestive of a shift towards tau-mediated neurodegeneration (Ballatore et al., 2007) in later stages of the disease or simply due to the smaller sample size available for analyses. Future studies additionally covarying for regional tau PET accumulation or extensions of studies investigating remote associations of pathologies (Tosun et al., 2017) may further elucidate the regional and spatial effects of cerebrovascular and both AD pathologies on regional neurodegeneration across different disease stages.

Across these regional analyses, we did not find evidence supportive of an interactive relationship between WMH and regional amyloid PET on regional cortical thickness. Interactive relationships were also not found when averaging Aβ and cortical thickness in known AD-associated regions into composite measures. This lack of regional interaction effects in the current study parallels findings from studies using global Aβ burden where interactive effects are weak or absent, especially in CN individuals (Gordon et al., 2015; Parker et al., 2020; Provenzano et al., 2013; Saridin et al., 2020). In line with a systematic review suggesting that Aβ accumulation and WMH are independent processes (Roseborough et al., 2017), our findings additionally suggest that these processes are independent even when investigated at regional levels of Aβ and neurodegeneration across disease stages.

Our longitudinal survival analyses revealed that global WMH, composite Aβ and composite cortical thickness in known AD-associated regions predicted progression to AD dementia in non-demented individuals and in MCI individuals alone. In both analyses, the hazard ratios of Aβ and cortical thickness were of comparable magnitude with each contributing to about 2.5 times higher risk of progression to AD dementia. In addition, although of a smaller magnitude, global WMH also independently contributed to greater risk of disease progression (~1.4 times). Taken together, our findings support the relevance of WMH as a vascular contribution to the AD process. These results builds upon recent findings (Calvin et al., 2020; Lam et al., 2021) suggesting that WMH may be useful as an additional vascular (V) biomarker in the AT(N) framework (Jack et al., 2018). In addition, given that vascular risk factors are largely modifiable, our results support the potential utility of modifying vascular dysfunction through

interventions (Sweeney et al., 2019) to reduce neurodegeneration and slow down progression to AD dementia.

This study is limited by the fact that ADNI participants with a modified Hachinski ischemic score (Rosen et al., 1980) of above 4 were excluded from the study, and therefore the eligible participants do not represent the entire spectrum of cerebrovascular disease severity. However, given that these relationships were still found in the current study suggest that even moderate presence of cerebrovascular disease can contribute significantly to regional neurodegeneration independent of regional Aβ burden. Although it is also likely that some of the WMH that we see is due to AD pathology resulting in Wallerian degeneration, post-mortem histological evidence suggests that for older controls, white matter lesions in parietal regions are likely due to ischemia and not AD-pathology (McAleese et al., 2017). While regional WMH data were not available on ADNI for analysis in the current study and that lesions in the white matter do not map directly to regional cortical Aβ and thickness measures, prior studies have found that regional WMH in frontal and parietal regions were associated with faster Aβ accumulation (Moscoso et al., 2020), that parietal WMH predicted progression to AD dementia (Brickman et al., 2015), and having larger posterior WMH volume was strongly associated with cognitive impairment (Garnier-Crussard et al., 2020). These regional WMH findings suggest that delineating gross regional WMH in the different cerebral lobes in future studies may provide further insights into the regional relationships between these neuroimaging biomarkers. In addition, the independent and interactive analyses were conducted cross-sectionally, future studies may be able to further elucidate potential longitudinal relationships of WMH and regional Aβ accumulation on the progression of regional cortical thinning. In CN individuals, although the associations of global WMH and regional Aβ did not survive correction for multiple comparisons, future studies may be able to validate these associations, particularly in the fronto-parietal regions where the effect sizes were the largest. Lastly, these results may not be generalizable to other populations as ADNI participants were recruited to reflect a clinical trial cohort, more than 90% of the participants in ADNI are White and with relatively high education levels.

In conclusion, the current study demonstrates that WMH contributes to regional neurodegeneration, independent of regional Aβ accumulation in different spatial regions as a function of clinical diagnosis – from fronto-temporal in CN individuals to temporal and cingulate regions in MCI individuals. In comparison, the independent influence of regional Aβ on regional neurodegeneration is muted in preclinical stages before manifestation in temporal regions in MCI individuals. The independent associations of global WMH beyond regional Aβ and cortical thickness in AD-associated regions on disease progression also supports the importance of cerebrovascular disease in the AD process. Taken together, our combined results suggest the need for a nuanced understanding of the relationships between WMH, Aβ accumulation and neurodegeneration, which may be regional, dynamic, and differ as a function of clinically diagnosed disease stage.

Disclosure statement

The author(s) declared no potential conflicts of interest with respect to the research, authorship, and/or publication of this article.

Acknowledgements

This study was supported by Nanyang Technological University, Singapore Start-Up Grant M40824100 (CHT) and MOE AcRF Tier 1 M4012193 (CHT). Data collection and sharing for this project was funded by the Alzheimer's Disease Neuroimaging Initiative (ADNI) (National Institutes of Health Grant U01 AG024904) and DOD ADNI (Department of Defense award number W81XWH-12-2-0012). ADNI is funded by the National Institute on Aging, the National Institute of Biomedical Imaging and Bioengineering, and through generous contributions from the following: AbbVie, Alzheimer's Association; Alzheimer's Drug Discovery Foundation; Araclon Biotech; BioClinica, Inc.; Biogen; Bristol-Myers Squibb Company; CereSpir, Inc.; Cogstate; Eisai Inc.; Elan Pharmaceuticals, Inc.; Eli Lilly and Company; EuroImmun; F. Hoffmann-La Roche Ltd and its affiliated company Genentech, Inc.; Fujirebio; GE Healthcare; IXICO Ltd.;Janssen Alzheimer Immunotherapy Research & Development, LLC.; Johnson & Johnson Pharmaceutical Research & Development LLC.; Lumosity; Lundbeck; Merck & Co., Inc.;Meso Scale Diagnostics, LLC.; NeuroRx Research; Neurotrack Technologies; Novartis Pharmaceuticals Corporation; Pfizer Inc.; Piramal Imaging; Servier; Takeda Pharmaceutical Company; and Transition Therapeutics. The Canadian Institutes of Health Research is providing funds to support ADNI clinical sites in Canada. Private sector contributions are facilitated by the Foundation for the National Institutes of Health (www.fnih.org). The grantee organization is the Northern California Institute for Research and Education, and the study is coordinated by the Alzheimer's Therapeutic Research Institute at the University of Southern California. ADNI data are disseminated by the Laboratory for Neuro Imaging at the University of Southern California.

Verification

The manuscript is not under consideration for publication elsewhere, that its publication is approved by all authors and tacitly or explicitly by the responsible authorities where the work was carried out, and that, if accepted, it will not be published elsewhere in the same form, in English or in any other language, including electronically without the written consent of the copyright-holder.

Supplementary materials

Supplementary material associated with this article can be found, in the online version, at doi:10.1016/j.neurobiolaging.2022.03.013.

REFERENCES

Ballatore, C., Lee, V.M.Y., Trojanowski, J.Q., 2007. Tau-mediated neurodegeneration in Alzheimer's disease and related disorders. Nature Reviews Neuroscience 8 (9), 663–672.

Benedictus, M.R., van Harten, A.C., Leeuwis, A.E., Koene, T., Scheltens, P., Barkhof, F., Prins, N.D., van der Flier, W.M., 2015. White matter hyperintensities relate to clinical progression in subjective cognitive decline. Stroke 46 (9), 2661–2664.

Bos, I., Verhey, F.R., Ramakers, I., Jacobs, H.I.L., Soininen, H., Freund-Levi, Y., Hampel, H., Tsolaki, M., Wallin, Å.K., van Buchem, M.A., Oleksik, A., Verbeek, M.M., Olde Rikkert, M., van der Flier, W.M., Scheltens, P., Aalten, P., Visser, P.J., Vos, S.J.B., 2017. Cerebrovascular and amyloid pathology in predementia stages: the relationship with neurodegeneration and cognitive decline. Alzheimers Res Ther 9 (1), 101.

Boyle, P.A., Yu, L., Wilson, R.S., Leurgans, S.E., Schneider, J.A., Bennett, D.A., 2018. Person-specific contribution of neuropathologies to cognitive loss in old age. Ann Neurol 83 (1), 74–83.

Brickman, A.M., Zahodne, L.B., Guzman, V.A., Narkhede, A., Meier, I.B., Griffith, E.Y., Provenzano, F.A., Schupf, N., Manly, J.J., Stern, Y., Luchsinger, J.A., Mayeux, R., 2015. Reconsidering harbingers of dementia: progression of parietal lobe white matter hyperintensities predicts Alzheimer's disease incidence. Neurobiol Aging 36 (1), 27–32.

Calvin, C.M., de Boer, C., Raymont, V., Gallacher, J., Koychev, I., 2020. Prediction of Alzheimer's disease biomarker status defined by the 'ATN framework' among cognitively healthy individuals: results from the EPAD longitudinal cohort study. Alzheimer's Research & Therapy 12 (1), 143.

Dadar, M., Camicioli, R., Duchesne, S., Collins, D.L., 2020. The temporal relationships between white matter hyperintensities, neurodegeneration, amyloid beta, and cognition. Alzheimers Dement (Amst) 12 (1), e12091.

Dadar, M., Manera, A.L., Ducharme, S., Collins, D.L., 2022. White matter hyperintensities are associated with grey matter atrophy and cognitive decline in Alzheimer's disease and frontotemporal dementia. Neurobiol Aging 111, 54–63.
Dale, A.M., Fischl, B., Sereno, M.I., 1999. Cortical Surface-Based Analysis: I. Segmentation and Surface Reconstruction. NeuroImage 9 (2), 179–194.
De Guio, F., Duering, M., Fazekas, F., De Leeuw, F.E., Greenberg, S.M., Pantoni, L., Aghetti, A., Smith, E.E., Wardlaw, J., Jouvent, E., 2020. Brain atrophy in cerebral small vessel diseases: Extent, consequences, technical limitations and perspectives: The HARNESS initiative. J Cereb Blood Flow Metab 40 (2), 231–245.
DeCarli, C., Fletcher, E., Ramey, V., Harvey, D., Jagust, W.J., 2005. Anatomical mapping of white matter hyperintensities (WMH): exploring the relationships between periventricular WMH, deep WMH, and total WMH burden. Stroke 36 (1), 50–55.
DeCarli, C., Murphy, D.G., Teichberg, D., Campbell, G., Sobering, G.S., 1996. Local histogram correction of MRI spatially dependent image pixel intensity nonuniformity. J Magn Reson Imaging 6 (3), 519–528.
Desikan, R.S., Segonne, F., Fischl, B., Quinn, B.T., Dickerson, B.C., Blacker, D., Buckner, R.L., Dale, A.M., Maguire, R.P., Hyman, B.T., Albert, M.S., Killiany, R.J., 2006. An automated labeling system for subdividing the human cerebral cortex on MRI scans into gyral based regions of interest. Neuroimage 31 (3), 968–980.
Dickerson, B.C., Bakkour, A., Salat, D.H., Feczko, E., Pacheco, J., Greve, D.N., Grodstein, F., Wright, C.I., Blacker, D., Rosas, H.D., Sperling, R.A., Atri, A., Growdon, J.H., Hyman, B.T., Morris, J.C., Fischl, B., Buckner, R.L., 2009. The cortical signature of Alzheimer's disease: regionally specific cortical thinning relates to symptom severity in very mild to mild AD dementia and is detectable in asymptomatic amyloid-positive individuals. Cereb Cortex 19 (3), 497–510.
Du, A.T., Schuff, N., Chao, L.L., Kornak, J., Ezekiel, F., Jagust, W.J., Kramer, J.H., Reed, B.R., Miller, B.L., Norman, D., Chui, H.C., Weiner, M.W., 2005. White matter lesions are associated with cortical atrophy more than entorhinal and hippocampal atrophy. Neurobiol Aging 26 (4), 553–559.
Fischl, B., Dale, A.M., 2000. Measuring the thickness of the human cerebral cortex from magnetic resonance images. Proc Natl Acad Sci U S A 97 (20), 11050–11055.
Garnier-Crussard, A., Bougacha, S., Wirth, M., André, C., Delarue, M., Landeau, B., Mézenge, F., Kuhn, E., Gonneaud, J., Chocat, A., Quillard, A., Ferrand-Devouge, E., de La Sayette, V., Vivien, D., Krolak-Salmon, P., Chételat, G., 2020. White matter hyperintensities across the adult lifespan: relation to age, Aβ load, and cognition. Alzheimers Res Ther 12 (1), 127.
Gordon, B.A., Najmi, S., Hsu, P., Roe, C.M., Morris, J.C., Benzinger, T.L., 2015. The effects of white matter hyperintensities and amyloid deposition on Alzheimer dementia. Neuroimage Clin 8, 246–252.
Grothe, M.J., Barthel, H., Sepulcre, J., Dyrba, M., Sabri, O., Teipel, S.J., 2017. In vivo staging of regional amyloid deposition. Neurology 89 (20), 2031–2038.
Habes, M., Erus, G., Toledo, J.B., Zhang, T., Bryan, N., Launer, L.J., Rosseel, Y., Janowitz, D., Doshi, J., Van der Auwera, S., von Sarnowski, B., Hegenscheid, K., Hosten, N., Homuth, G., Völzke, H., Schminke, U., Hoffmann, W., Grabe, H.J., Davatzikos, C., 2016. White matter hyperintensities and imaging patterns of brain ageing in the general population. Brain 139 (Pt 4), 1164–1179.
Heng, L.C., Lim, S.H., Foo, H., Kandiah, N., 2021. Confluent white matter in progression to alzheimer dementia. Alzheimer Dis Assoc Disord 35 (1), 8–13.
Jack, C.R., Bennett, D.A., Blennow, K., Carrillo, M.C., Dunn, B., Haeberlein, S.B., Holtzman, D.M., Jagust, W., Jessen, F., Karlawish, J., Liu, E., Molinuevo, J.L., Montine, T., Phelps, C., Rankin, K.P., Rowe, C.C., Scheltens, P., Siemers, E., Snyder, H.M., Sperling, R., 2018. NIA-AA research framework: toward a biological definition of Alzheimer's disease. Alzheimers Dement 14 (4), 535–562.
Kan, C.N., Xu, X., Schmetterer, L., Venketasubramanian, N., Chen, C., Tan, C.H., 2022. Interactions of comorbid neuropsychiatric subsyndromes with neurodegenerative and cerebrovascular pathologies on cognition. Neurobiology of Aging 109, 239–246.
Kim, S., Choi, S.H., Lee, Y.M., Kim, M.J., Kim, Y.D., Kim, J.Y., Park, J.H., Myung, W., Na, H.R., Han, H.J., Shim, Y.S., Kim, J.H., Yoon, S.J., Kim, S.Y., Kim, D.K., 2015. Periventricular white matter hyperintensities and the risk of dementia: a CREDOS study. Int Psychogeriatr 27 (12), 2069–2077.
Kim, S.J., Lee, D.K., Jang, Y.K., Jang, H., Kim, S.E., Cho, S.H., Kim, J.P., Jung, Y.H., Kim, E.J., Na, D.L., Lee, J.M., Seo, S.W., Kim, H.J., 2020. The effects of longitudinal white matter hyperintensity change on cognitive decline and cortical thinning over three years. J Clin Med 9 (8), 2663.
Lam, S., Lipton, R.B., Harvey, D.J., Zammit, A.R., Ezzati, A., 2021. White matter hyperintensities and cognition across different Alzheimer's biomarker profiles. J Am Geriatr Soc 69 (7), 1906–1915.
Landau, S.M., Lu, M., Joshi, A.D., Pontecorvo, M., Mintun, M.A., Trojanowski, J.Q., Shaw, L.M., Jagust, W.J., 2013. Comparing positron emission tomography imaging and cerebrospinal fluid measurements of β-amyloid. Ann Neurol 74 (6), 826–836.
Landau, S.M., Mintun, M.A., Joshi, A.D., Koeppe, R.A., Petersen, R.C., Aisen, P.S., Weiner, M.W., Jagust, W.J., 2012. Amyloid deposition, hypometabolism, and longitudinal cognitive decline. Ann Neurol 72 (4), 578–586.
Lao, P.J., Brickman, A.M., 2018. Multimodal neuroimaging study of cerebrovascular disease, amyloid deposition, and neurodegeneration in Alzheimer's disease progression. Alzheimers Dement (Amst) 10, 638–646.
Lyketsos, C.G., Lopez, O., Jones, B., Fitzpatrick, A.L., Breitner, J., DeKosky, S., 2002. Prevalence of neuropsychiatric symptoms in dementia and mild cognitive impairment results from the cardiovascular health study. JAMA 288 (12), 1475–1483.
Mattsson, N., Palmqvist, S., Stomrud, E., Vogel, J., Hansson, O., 2019. Staging β-Amyloid pathology with amyloid positron emission tomography. JAMA Neurol 76 (11), 1319–1329.
McAleese, K.E., Walker, L., Graham, S., Moya, E.L.J., Johnson, M., Erskine, D., Colloby, S.J., Dey, M., Martin-Ruiz, C., Taylor, J.P., Thomas, A.J., McKeith, I.G., De Carli, C., Attems, J., 2017. Parietal white matter lesions in Alzheimer's disease are associated with cortical neurodegenerative pathology, but not with small vessel disease. Acta Neuropathol 134 (3), 459–473.
Misquitta, K., Dadar, M., Louis Collins, D., Tartaglia, M.C., 2020. White matter hyperintensities and neuropsychiatric symptoms in mild cognitive impairment and Alzheimer's disease. Neuroimage Clin 28, 102367.
Moscoso, A., Rey-Bretal, D., Silva-Rodríguez, J., Aldrey, J.M., Cortés, J., Pías-Peleteiro, J., Ruibal, Á., Aguiar, P., 2020. White matter hyperintensities are associated with subthreshold amyloid accumulation. Neuroimage 218, 116944.
Ossenkoppele, R., Schonhaut, D.R., Schöll, M., Lockhart, S.N., Ayakta, N., Baker, S.L., O'Neil, J.P., Janabi, M., Lazaris, A., Cantwell, A., Vogel, J., Santos, M., Miller, Z.A., Bettcher, B.M., Vossel, K.A., Kramer, J.H., Gorno-Tempini, M.L., Miller, B.L., Jagust, W.J., Rabinovici, G.D., 2016. Tau PET patterns mirror clinical and neuroanatomical variability in Alzheimer's disease. Brain 139 (Pt 5), 1551–1567.
Parker, T.D., Cash, D.M., Lane, C.A., Lu, K., Malone, I.B., Nicholas, J.M., James, S.N., Keshavan, A., Murray-Smith, H., Wong, A., Buchanan, S.M., Keuss, S.E., Sudre, C.H., Thomas, D.L., Crutch, S.J., Fox, N.C., Richards, M., Schott, J.M., 2020. Amyloid β influences the relationship between cortical thickness and vascular load. Alzheimers Dement (Amst) 12 (1), e12022.
Pfeil, J., Hoenig, M.C., Doering, E., van Eimeren, T., Drzezga, A., Bischof, G.N., 2021. Unique regional patterns of amyloid burden predict progression to prodromal and clinical stages of Alzheimer's disease. Neurobiol Aging 106, 119–129.
Provenzano, F.A., Muraskin, J., Tosto, G., Narkhede, A., Wasserman, B.T., Griffith, E.Y., Guzman, V.A., Meier, I.B., Zimmerman, M.E., Brickman, A.M., 2013. White Matter Hyperintensities and Cerebral Amyloidosis: Necessary and Sufficient for Clinical Expression of Alzheimer Disease? JAMA Neurology 70 (4), 455–461.
Rizvi, B., Lao, P.J., Chesebro, A.G., Dworkin, J.D., Amarante, E., Beato, J.M., Gutierrez, J., Zahodne, L.B., Schupf, N., Manly, J.J., Mayeux, R., Brickman, A.M., 2021. Association of Regional White Matter Hyperintensities With Longitudinal Alzheimer-Like Pattern of Neurodegeneration in Older Adults. JAMA Network Open 4 (10), e2125166.
Roseborough, A., Ramirez, J., Black, S.E., Edwards, J.D., 2017. Associations between amyloid β and white matter hyperintensities: A systematic review. Alzheimers Dement 13 (10), 1154–1167.
Rosen, W.G., Terry, R.D., Fuld, P.A., Katzman, R., Peck, A., 1980. Pathological verification of ischemic score in differentiation of dementias. Ann Neurol 7 (5), 486–488.
Sanchez, J.S., Becker, J.A., Jacobs, H.I.L., Hanseeuw, B.J., Jiang, S., Schultz, A.P., Properzi, M.J., Katz, S.R., Beiser, A., Satizabal, C.L., O'Donnell, A., DeCarli, C., Killiany, R., El Fakhri, G., Normandin, M.D., Gómez-Isla, T., Quiroz, Y.T., Rentz, D.M., Sperling, R.A., Seshadri, S., Augustinack, J., Price, J.C., Johnson, K.A., 2021. The cortical origin and initial spread of medial temporal tauopathy in Alzheimer's disease assessed with positron emission tomography. Sci Transl Med 13 (577), eabc0655.
Saridin, F.N., Hilal, S., Villaraza, S.G., Reilhac, A., Gyanwali, B., Tanaka, T., Stephenson, M.C., Ng, S.L., Vrooman, H., van der Flier, W.M., Chen, C.L.H., 2020. Brain amyloid β, cerebral small vessel disease, and cognition: a memory clinic study. Neurology 95 (21), e2845–e2853.
Schwarz, C.G., Gunter, J.L., Wiste, H.J., Przybelski, S.A., Weigand, S.D., Ward, C.P., Senjem, M.L., Vemuri, P., Murray, M.E., Dickson, D.W., Parisi, J.E., Kantarci, K., Weiner, M.W., Petersen, R.C., Jack, C.R., 2016. A large-scale comparison of cortical thickness and volume methods for measuring Alzheimer's disease severity. Neuroimage Clin 11, 802–812.
Sepulcre, J., Schultz, A.P., Sabuncu, M., Gomez-Isla, T., Chhatwal, J., Becker, A., Sperling, R., Johnson, K.A., 2016. In Vivo Tau, Amyloid, and Gray Matter Profiles in the Aging Brain. J Neurosci 36 (28), 7364–7374.
Sweeney, M.D., Montagne, A., Sagare, A.P., Nation, D.A., Schneider, L.S., Chui, H.C., Harrington, M.G., Pa, J., Law, M., Wang, D.J.J., Jacobs, R.E., Doubal, F.N., Ramirez, J., Black, S.E., Nedergaard, M., Benveniste, H., Dichgans, M., Iadecola, C., Love, S., Bath, P.M., Markus, H.S., Salman, R.A., Allan, S.M., Quinn, T.J., Kalaria, R.N., Werring, D.J., Carare, R.O., Touyz, R.M., Williams, S.C.R., Moskowitz, M.A., Katusic, Z.S., Lutz, S.E., Lazarov, O., Minshall, R.D., Rehman, J., Davis, T.P., Wellington, C.L., González, H.M., Yuan, C., Lockhart, S.N., Hughes, T.M., Chen, C.L.H., Sachdev, P., O'Brien, J.T., Skoog, I., Pantoni, L., Gustafson, D.R., Biessels, G.J., Wallin, A., Smith, E.E., Mok, V., Wong, A., Passmore, P., Barkof, F., Muller, M., Breteler, M.M.B., Román, G.C., Hamel, E., Seshadri, S., Gottesman, R.F., van Buchem, M.A., Arvanitakis, Z., Schneider, J.A., Drewes, L.R., Hachinski, V., Finch, C.E., Toga, A.W., Wardlaw, J.M., Zlokovic, B.V., 2019. Vascular dysfunction-The disregarded partner of Alzheimer's disease. Alzheimers Dement 15 (1), 158–167.
Tan, C.H., Fan, C.C., Mormino, E.C., Sugrue, L.P., Broce, I.J., Hess, C.P., Dillon, W.P., Bonham, L.W., Yokoyama, J.S., Karch, C.M., Brewer, J.B., Rabinovici, G.D., Miller, B.L., Schellenberg, G.D., Kauppi, K., Feldman, H.A., Holland, D., McEvoy, L.K., Hyman, B.T., Bennett, D.A., Andreassen, O.A., Dale, A.M., Desikan, R.S., 2018. Polygenic hazard score: an enrichment marker for Alzheimer's associated amyloid and tau deposition. Acta Neuropathol 135 (1), 85–93.
Tan, C.H., Hyman, B.T., Tan, J.J.X., Hess, C.P., Dillon, W.P., Schellenberg, G.D., Besser, L.M., Kukull, W.A., Kauppi, K., McEvoy, L.K., Andreassen, O.A., Dale, A.M.,

Fan, C.C., Desikan, R.S., 2017. Polygenic hazard scores in preclinical Alzheimer disease. Ann Neurol 82 (3), 484–488.
Tan, C.H., Low, K.A., Chiarelli, A.M., Fletcher, M.A., Navarra, R., Burzynska, A.Z., Kong, T.S., Zimmerman, B., Maclin, E.L., Sutton, B.P., Gratton, G., Fabiani, M., 2019. Optical measures of cerebral arterial stiffness are associated with white matter signal abnormalities and cognitive performance in normal aging. Neurobiol Aging 84, 200–207.
Tosun, D., Landau, S., Aisen, P.S., Petersen, R.C., Mintun, M., Jagust, W., Weiner, M.W., 2017. Association between tau deposition and antecedent amyloid-β accumulation rates in normal and early symptomatic individuals. Brain 140 (5), 1499–1512.
Tuladhar, A.M., Reid, A.T., Shumskaya, E., de Laat, K.F., van Norden, A.G., van Dijk, E.J., Norris, D.G., de Leeuw, F.E., 2015. Relationship between white matter hyperintensities, cortical thickness, and cognition. Stroke 46 (2), 425–432.
Vipin, A., Foo, H.J.L., Lim, J.K.W., Chander, R.J., Yong, T.T., Ng, A.S.L., Hameed, S., Ting, S.K.S., Zhou, J., Kandiah, N., 2018. Regional white matter hyperintensity influences grey matter atrophy in mild cognitive impairment. J Alzheimers Dis 66 (2), 533–549.
Yassi, N., Hilal, S., Xia, Y., Lim, Y.Y., Watson, R., Kuijf, H., Fowler, C., Yates, P., Maruff, P., Martins, R., Ames, D., Chen, C., Rowe, C.C., Villemagne, V.L., Salvado, O., Desmond, P.M., Masters, C.L., 2020. Influence of comorbidity of cerebrovascular disease and Amyloid-β on Alzheimer's Disease. J Alzheimers Dis 73 (3), 897–907.
Ye, B.S., Seo, S.W., Kim, G.H., Noh, Y., Cho, H., Yoon, C.W., Kim, H.J., Chin, J., Jeon, S., Lee, J.M., Seong, J.K., Kim, J.S., Lee, J.H., Choe, Y.S., Lee, K.H., Sohn, Y.H., Ewers, M., Weiner, M., Na, D.L., 2015. Amyloid burden, cerebrovascular disease, brain atrophy, and cognition in cognitively impaired patients. Alzheimers Dement 11 (5), 494–503 e493.
Zhao, Q.F., Tan, L., Wang, H.F., Jiang, T., Tan, M.S., Tan, L., Xu, W., Li, J.Q., Wang, J., Lai, T.J., Yu, J.T., 2016. The prevalence of neuropsychiatric symptoms in Alzheimer's disease: Systematic review and meta-analysis. J Affect Disord 190, 264–271.
Zhu, D.C., Majumdar, S., Korolev, I.O., Berger, K.L., Bozoki, A.C., 2013. Alzheimer's disease and amnestic mild cognitive impairment weaken connections within the default-mode network: a multi-modal imaging study. J Alzheimers Dis 34 (4), 969–984.